21st Australasian Fluid Mechanics Conference
Adelaide, Australia
10-13 December 2018

Shock Interactions in Multi-Fluid Plasmas

D. Bond[1], V. Wheatley[1], S. Imran[1], R. Samtaney[2], D. Pullin[3], Y. Li[2]

[1]School of Mechanical and Mining Engineering
The University of Queensland, St Lucia, Queensland 4072, Australia

[2]Mechanical Engineering, King Abdullah University of Science and Technology, Thuwal, Saudi Arabia

[3]Graduate Aerospace Laboratories, California Institute of Technology, Pasadena, California 91125, USA

Abstract

Shock interactions in plasmas can occur in settings as varied as stellar physics, inertial confinement fusion experiments and planetary entry of spacecraft. In unmagnetised plasmas, shock interactions with density discontinuities typically result in vorticity being deposited on the discontinuity, driving interfacial instability. In the context of fusion, such instabilities are highly detrimental to performance. In the magneto-hydrodynamic limit, it has been theoretically demonstrated that in a magnetized plasma the structure of the shock interaction usually changes such that vorticity is transported from the discontinuity, resulting in the suppression of interfacial shear instabilities. This suppression is potentially beneficial in inertial confinement fusion experiments. The magneto-hydrodynamic limit, however, only applies if the plasma length scales are small in comparison to the length-scales characterizing the problem of interest. This allows effects including charge separation, self-generated electric and magnetic fields and a host of wave phenomena to be neglected. In the present work, the influence of finite plasma length-scales on shock interactions in magnetized and unmagnetised plasmas is explored computationally.

Introduction

A plasma may be mathematically described via a hierarchy of models, starting with a kinetic view of the individual particles (ions, electrons, neutrals) and progressing to the magneto-hydrodynamic (MHD) approximation. The MHD model is prevalent in numerical plasma flow investigation but does not account for effects that become apparent when plasma length scales are appreciable when compared to the scale of the problem of interest. In this case alternative models may be used of which the ideal two-fluid approximation is one [1, 2, 3, 4].

Clean power generation through the process of inertial confinement fusion (ICF) has inspired significant research into modelling the dynamics of plasma implosions in which hydrodynamic instabilities comprise a major role [6]. The suppression of the Richtmyer-Meshkov instability (RMI) of a shock-accelerated density interface through the application of an initial magnetic field has been theoretically demonstrated [9, 10] whereby the vorticity generated at the density interface during the shock interaction is transported away by MHD waves. In this work the vorticity transport dynamics resulting from shock-density interface interactions are investigated over a range of plasma regimes under the two-fluid plasma approximation such that finite plasma length scale effects may be observed.

Two fluid model equations

The ideal five-moment evolution equations for an ion-electron plasma are formed by the coupling of the Euler fluid equations for each species, with appropriate source terms for electromagnetic effects, and Maxwell's equations for electromagnetism [5, 2]. Here we will show these equations in their non-dimensional form following Bond *et. al* [4, 3].

Equations of fluid motion

The Euler equations for ions and electrons along with contributions from electromagnetic fields are shown below in non-dimensional form,

$$\begin{aligned}
\frac{\partial \rho_\alpha}{\partial t} + \nabla\cdot(\rho_\alpha \mathbf{u}_\alpha) &= 0,\\
\frac{\partial \rho_\alpha \mathbf{u}_\alpha}{\partial t} + \nabla\cdot(\rho_\alpha \mathbf{u}_\alpha \mathbf{u}_\alpha + p_\alpha \mathbf{I}) &= \frac{\rho_\alpha r_\alpha}{d_{L,0}}\left(c\mathbf{E} + \mathbf{u}_\alpha \times \mathbf{B}\right),\\
\frac{\partial \varepsilon_\alpha}{\partial t} + \nabla\cdot\left((\varepsilon_\alpha + p_\alpha)\,\mathbf{u}_\alpha\right) &= \frac{\rho_\alpha r_\alpha c}{d_{L,0}}\mathbf{u}_\alpha\cdot\mathbf{E},
\end{aligned}$$

where

$$\rho_\alpha = m_\alpha n_\alpha \qquad r_\alpha = \frac{q_\alpha}{m_\alpha}, \qquad \varepsilon_\alpha = \frac{p_\alpha}{\gamma - 1} + \frac{\rho_\alpha \mathbf{u}_\alpha\cdot\mathbf{u}_\alpha}{2}.$$

In these equations we evolve density ρ, pressure p, velocity $\mathbf{u}$ and energy ε with respect to time t. Source terms include electric field $\mathbf{E}$, magnetic field $\mathbf{B}$, speed of light c, reference Larmor radius $d_{L,0}$ and Debye length $d_{D,0}$. The species, ions or electrons, is denoted by subscript α while the mass and charge is given by m and q.

Electromagnetic evolution

The evolution of the electromagnetic fields is intrinsically linked to the species evolution through the modified Maxwell's equations [7],

$$\begin{aligned}
\frac{\partial \mathbf{E}}{\partial t} - c\nabla\times\mathbf{B} + c\Gamma_E\nabla\psi_E &= -\frac{d_{L,0}}{d_{D,0}^2 c}\sum_\alpha \rho_\alpha r_\alpha \mathbf{u}_\alpha,\\
\frac{\partial \mathbf{B}}{\partial t} + c\nabla\times\mathbf{E} + c\Gamma_B\nabla\psi_B &= 0,\\
\frac{\partial \psi_E}{\partial t} + \Gamma_E c\nabla\cdot\mathbf{E} &= \frac{d_{L,0}\Gamma_E}{d_{D,0}^2}\sum_\alpha r_\alpha\rho_\alpha,\\
\frac{\partial \psi_B}{\partial t} + c\Gamma_B\nabla\cdot\mathbf{B} &= 0,
\end{aligned}$$

where ψ_E and ψ_B are Lagrange multipliers introduced to drive errors in the divergence of $\mathbf{E}$ and $\mathbf{B}$ to zero. This approach main-

tains a hyperbolic formulation with wave speeds for these correction quantities of Γ_E and Γ_B respectively.

Plasma regime definition

The reference Larmor radius and Debye length are used to dictate the plasma regime which is being simulated while β describes the impact of the electromagnetic fields on the fluid dynamics,

$$d_{D,0} = \sqrt{\frac{u_0^2 m_0}{c^2 \mu_0 n_0 q_0^2 x_0^2}}, \quad d_{L,0} = \frac{u_0 m_0}{q_0 B_0 x_0}, \quad \beta = \frac{d_{L,0}^2}{d_{D,0}^2 c^2} \frac{2p}{B^2}.$$

These terms include reference values for number density n_0, mass m_0, charge q_0, magnetic field B_0, length scale x_0, velocity u_0 and permeability of free space μ_0.

Implementation

Solutions to this set of equations were obtained numerically in two dimensional domains using a solver built on the adaptive mesh refinement framework Chombo. The numerical solver is a spatially second order accurate finite-volume scheme with a two-stage Runge–Kutta time integrator [5]. Fluxes are calculated via approximate Riemann solvers with HLLC for species and HLLE for electromagnetic fields. Source terms are solved for implicitly [1]. Verification of the solver has been carried out by Bond *et. al* [4, 3].

Initial conditions

To investigate the interaction of a shock with an inclined density interface the following initial conditions were used. In the ion species a Mach 2 shock was defined according to the Rankine–Hugoniot conditions. A density interface with ratio 3:1 (right to left) was then implemented with slope angle of 10 degrees relative to vertical and wave length of 2. This interface had a smooth hyperbolic tangent transition such that 90% of the variation was found over a distance of 0.01 units and was located with its maximum x location being 0.2 units upstream of the ion shock initial position. The electron species was initialised to give zero net charge at all points in the domain ($n_i = n_e$) and with a velocity equal to the ions. This initial condition may be described according to the three conditions S_0, S_1, and S_2 shown in figure 1 and given below for the ions,

$$\begin{pmatrix} \rho \\ p \\ u_x \\ u_y, u_z \end{pmatrix}_{i,S_0} = \begin{pmatrix} 2.286 \\ 2.375 \\ 1.027 \\ 0 \end{pmatrix}, \begin{pmatrix} \rho \\ p \\ \mathbf{u} \end{pmatrix}_{i,S_1} = \begin{pmatrix} 1 \\ 0.5 \\ \mathbf{0} \end{pmatrix}, \begin{pmatrix} \rho \\ p \\ \mathbf{u} \end{pmatrix}_{i,S_2} = \begin{pmatrix} 3 \\ 0.5 \\ \mathbf{0} \end{pmatrix}.$$

The electron density is then given by $\rho_e = (m_e/m_i)\,\rho_i$ while all other electron quantities are identical to the ions. The mass ratio was set to 100 with $m_i = 1$ and $m_e = 0.01$. Charge was set to $q_i = 1$ and $q_e = -1$. The ratio of specific heats for each species was set to $\gamma = 5/3$as appropriate for a fully ionised plasma. In order to vary the plasma regime the non-dimensional reference Debye length was varied according to $0.001 \leq d_{D,0} \leq 0.05$ while $d_{L,0} = 0.01$. In order to investigate the effect of magnetic fields on the shock-interface interaction an $x-$ aligned magnetic field was initialised with strength determined by the interaction

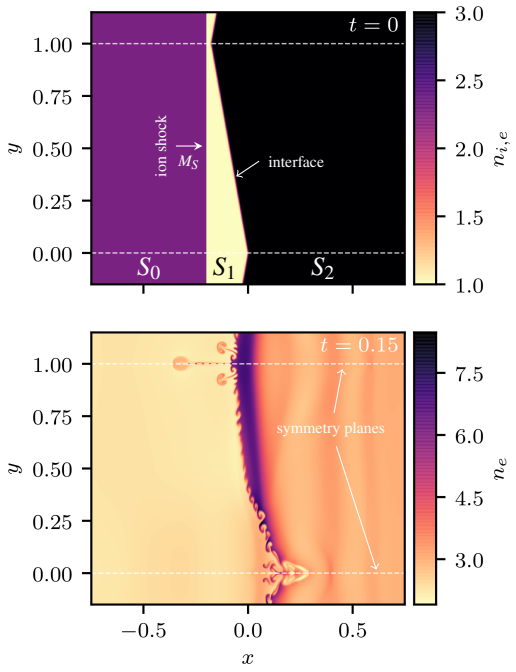

Figure 1: Initial and evolved number density of the triangular wave thermal interface for $d_{D,0} = 0.1$ and $\beta = \infty$. Initial condition composed of three states S_0, S_1, and S_2 with simulation domain bounded by planes of symmetry in y.

parameter β, in this case β had two values, $\beta = 0.01$ to correspond with a strong initial field, and $\beta = \infty$ for no initial field. The non-dimensional speed of light was set to $c = 50$ and divergence control parameters were $\Gamma_E = \Gamma_B = 1$.

The computational domain consisted of a base grid with 831×8 square cells with $\Delta x = 0.125$. The domain length was chosen to ensure that no speed of light waves would impact the x boundaries and thus introduce spurious waves over the course of the simulation. The domain was then allowed to refine over four levels with refinement ratios of four giving a maximum effective resolution of 512 cells per unit length. Boundary conditions in x were zero gradient while in y symmetry conditions were implemented for hydrodynamic quantities where the electric and magnetic fields had symmetric and anti-symmetric boundary conditions respectively.

Results

The results from our numerical experiments will be now discussed for each plasma regime simulated where each regime was investigated with and without an initial magnetic field. All results are for a time of $t = 0.2$ unless otherwise specified.

For all cases we observe a reflected and transmitted shock about the density interface along with perturbations to the ion flow due to relative electron fluid motion for larger $d_{D,0}$, the latter is particularly evident in the lower half of figure 2. However, the focus of this work is on the mitigation of interface instability which requires that we investigate the vorticity field about the interface. As the shock processes the density interface vorticity is generated due to baroclinic torque as described in equation 1 and observed in figures 2 through 6.

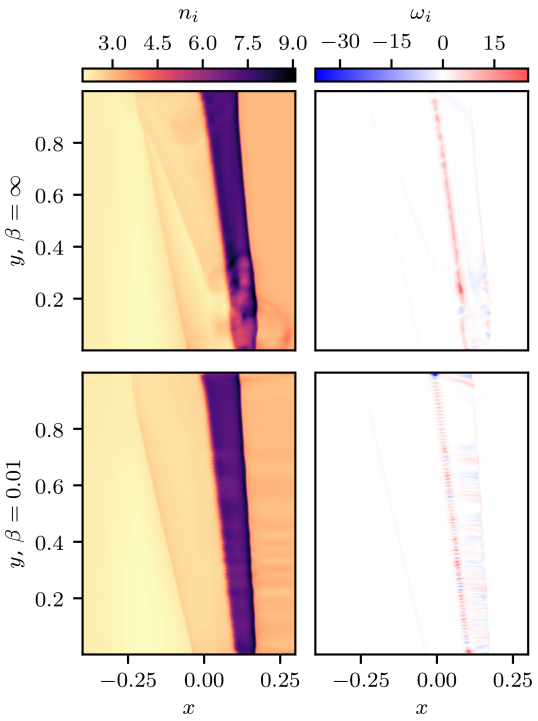

Figure 2: $d_{D,0} = 0.05$

$$\frac{\partial \omega_\alpha}{\partial t} \underbrace{- \nabla \times (\mathbf{u}_\alpha \times \omega_\alpha)}_{\text{vorticity transport}} \underbrace{- \frac{1}{\rho_\alpha^2} (\nabla \rho_\alpha \times \nabla p_\alpha)}_{\text{baroclinic torque}} = \nabla \times \underbrace{\left(\frac{r_\alpha}{d_L} (c\mathbf{E} + \mathbf{u}_\alpha \times \mathbf{B}) \right)}_{\text{Lorentz acceleration}} \quad (1)$$

For the initially unmagnetised cases this vorticity is seen to remain with the interface promoting deformation and, over longer time frames, leads to the classic bubble and spike behaviour (not shown). Introducing an initial magnetic field, as shown in the lower panels of the presented figures, introduces significant changes to the vorticity dynamics. Starting with $d_{D,0} = 0.05$ we observe the vorticity distribution along the interface becomes granular with closely spaced pockets of opposite sign. This is due to the disruptive effect of electrons being confined to move along magnetic fields lines as shown in figure 3 at $t = 0.5$.

As the reference Debye length decreases further this electron filamentation reduces in scale until it is filtered out of simulation by the grid resolution. The stabilising effect of the magnetic field is then observed in figure 4 where the ion interface displays minimal distortion. It can be observed that the sign of the vorticity on the interface has reversed in the presence of the field. This is part of a periodic oscillation of vorticity driven by the Lorentz term in the vorticity equation. Vorticity transport, due to the initial magnetic field, is also shown in the form of broad bands of vorticity being swept away from the interface.

For $d_{D,0} = 0.005$ this vorticity transport becomes stronger as shown in figure 5. Here we can more clearly see that the sign of vorticity on the interface oscillates about zero with stronger waves being transported away leaving the ion interface essentially stable as shown.

The increasing effectiveness of vorticity transport with decreasing plasma length scales becomes apparent when viewing figure 6. Here the diffuse bands of transported vorticity observed for larger $d_{D,0}$ become concentrated into localised wave packets with vorticity transport concentrated into waves departing the interface shortly after shock interaction and reduced transport thereafter. At this plasma length scale the vorticity is removed from the interface quite rapidly leading to a stabilised interface.

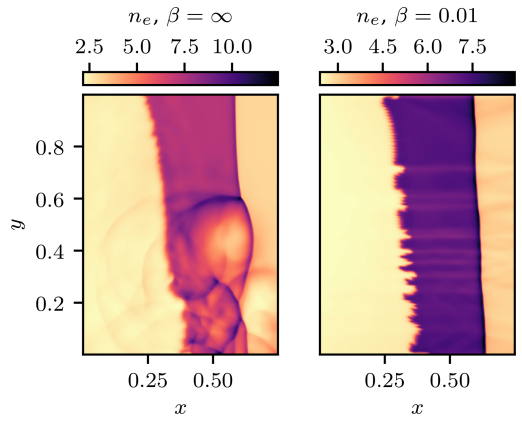

Figure 3: Electron dynamics for $d_{D,0} = 0.05$ at $t = 0.5$

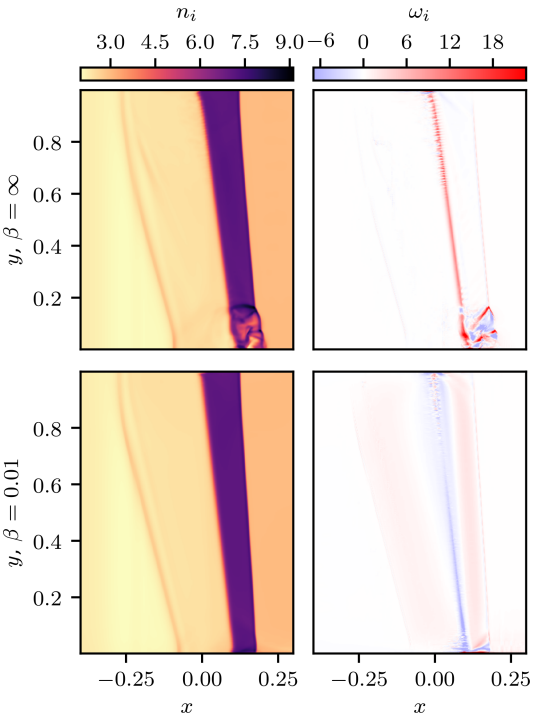

Figure 4: $d_{D,0} = 0.01$

Vorticity transport and reversal in two-fluid plasmas is due to the action of the Lorentz force as described by equation 1 and shown in 7 where the vertical acceleration of the ion fluid due to the action of the magnetic field is seen to closely correspond with the vorticity distribution.

Conclusions

The transport of vorticity away from the density interface of a shock driven RMI has been shown for magneto-hydrodynamic (MHD) plasma flows [8]. The two-fluid description of a plasma gives a framework for simulating plasmas ranging from hydrodynamic to quasi-neutral (MHD) in nature. In this work the

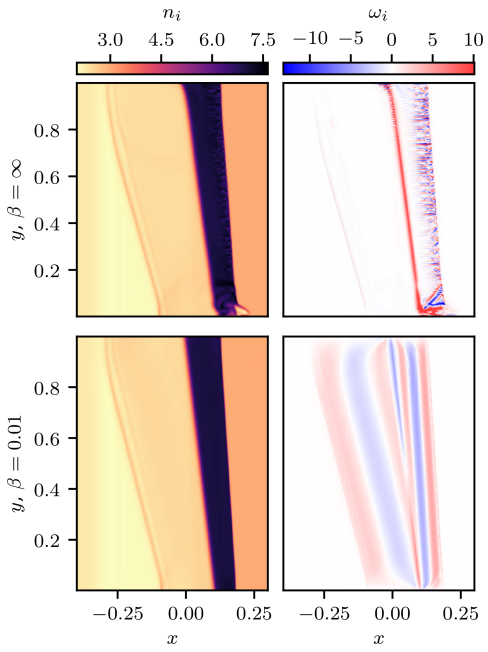

Figure 5: $d_{D,0} = 0.005$

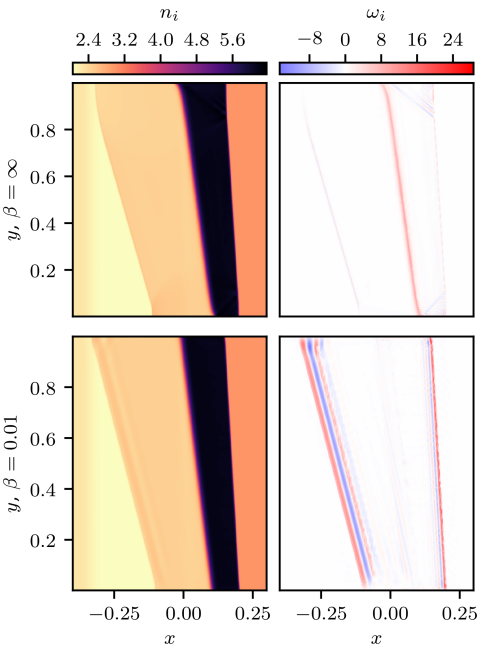

Figure 6: $d_{D,0} = 0.001$

suppression of the RMI through the application of an initial magnetic field has been demonstrated over a range of plasma regimes. At larger plasma length scales this suppression is due to sign reversal in vorticity and as scales decrease vorticity is increasingly transported away from the interface in a manner that converges towards MHD like behaviour. Thus it is observed that instability suppression due to the presence of an initial magnetic field is present across all plasma regimes but with varying mechanisms and effectiveness. These findings provide confidence in the results from the more approximate MHD model and support the use of initial magnetic fields in the suppression of hydrodynamic instabilities, such as the RMI, in plasma flows.

Acknowledgements

This research was supported by the KAUST Office of Sponsored Research under award URF/1/3418-01. This research was undertaken with the assistance of resources and services from the National Computational Infrastructure (NCI), which is supported by the Australian Government.

References

[1] Abgrall, R. and Kumar, H., Robust finite volume schemes for two-fluid plasma equations, *J. Sci. Comput.*, **60**, 2014, 584–611.

[2] Bellan, P. M., *Fundamentals of Plasma Physics*, Cambridge University Press, 2006.

[3] Bond, D., Wheatley, V., Samtaney, R. and Pullin, D. I., Richtmyer-Meshkov instability of a thermal interface in a two-fluid plasma, *Journal of Fluid Mechanics*, **833**, 2017, 332–363.

[4] Bond, D. M. and Samtaney, V. W. W., Plasma flow simulation using the two-fluid model, in *20th Australasian Fluid Mechanics Conference, Perth, Asutralia*, 2016.

[5] Goedbloed, J. P. and Poedts, S., *Principles of Magnetohydrodynamics: With Applications to Laboratory and Astrophysical Plasmas*, Cambridge University Press, 2004.

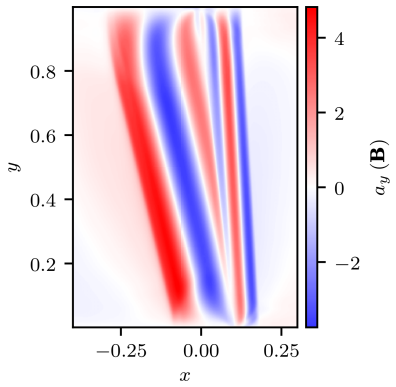

Figure 7: y component of acceleration due to magnetic field for $d_{D,0} = 0.005$. Note that the x component of acceleration displays the same general distribution but with significantly reduced magnitude ($\max(a_x(\mathbf{B})) \approx 0.006$)

[6] Lindl, J., Landen, O., Edwards, J. and Moses, E., Review of the National Ignition Campaign 2009-2012, *Physics of Plasmas*, **21**, 2014, 020501.

[7] Munz, C. D., Schneider, R. and Voss, U., A finite-volume method for the Maxwell equations in the time domain, *SIAM Journal on Scientific Computing*, **22**, 2000, 449–475.

[8] Samtaney, R., Suppression of the Richtmyer-Meshkov instability in the presence of a magnetic field, *Physics of Fluids*, **15**, 2003, L53–L56.

[9] Wheatley, V., Pullin, D. I. and Samtaney, R., Regular shock refraction at an oblique planar density interface in magnetohydrodynamics, *Journal of Fluid Mechanics*, **522**, 2005, 179–214.

[10] Wheatley, V., Pullin, D. I. and Samtaney, R., Stability of an impulsively accelerated density interface in magnetohydrodynamics, *Phys. Rev. Lett.*, **95**, 2005, 125002.